Magnetic-Field-Induced Surface States in Bismuth

J. F. KOCH
Department of Physics and Astronomy, University of Maryland, College Park, Maryland 20742

AND

J. D. JENSEN
Naval Ordnance Laboratory, White Oak, Maryland

(Received 20 January 1969)

The microwave-impedance oscillations observed in Bi single crystals in a weak magnetic field (0–6 Oe at 32 GHz) are due to resonant transitions between surface quantum states. After a brief "minimal theory" description of such surface states, we present a detailed calculation of the surface impedance spectrum for Bi that allows us to accurately evaluate Fermi-surface parameters from the experimental data. Using the established Fermi-surface geometry of Bi, we determine the Fermi velocity, point by point, on the central cross section of the electron ellipsoid to an accuracy of better than 2%. Values range from a maximum of 10.1×10^7 cm/sec in the binary (C_2) direction down to 7.8×10^7 cm/sec at right angles to C_2. A line integral of the velocities around the cross section agrees exactly with the cyclotron mass, $(0.0077\pm0.0002)m_0$, as measured in the present experiments. The accurately known Fermi surface of Bi has made it possible for us to explore and verify interesting geometrical features of the resonance signals.

I. INTRODUCTION

IN the presence of a magnetic field, electrons are bound to the surface region in skipping trajectories. Such electrons move along the surface by periodic specular reflection and form a system of quantum mechanical surface states.[1,2] Resonant transitions between the surface states account for the curious microwave impedance oscillations in weak magnetic fields that have been observed experimentally for many years.[3–8] A recent calculation[9,10] of the impedance spectrum and the very good agreement with representative experimental curves provide convincing confirmation of this interpretation.

The present Bi experiments were motivated by an effort to critically examine the dependence on Fermi-surface parameters in the theory, as well as to explore some geometrical aspects on hand of the well-established Fermi-surface configuration. Measurements of the surface-state resonances, together with available geometrical Fermi-surface information, yield point-by-point values of the Fermi velocity. We have aimed to make such determinations at points around the smallest central cross section of the ellipsoidal electron surface. In addition, the Bi data provide a proving ground for detailed line shape calculations, because one can hope to tackle the "k_y broadening" problem that has been ignored in previous calculations.[9]

The observation of surface quantum states in Bi also provides eloquent and unimpeachable proof of specular scattering of electrons at the surface. This had been surmised in various different transport experiments in Bi. The sensitive dependence of the resonances on the condition of the surface, however, should convince the reader that such specularity is to be achieved only with careful preparation and treatment of the surface.

The first observations of the weak-field impedance oscillations in Bi were reported by Khaikin.[6] However, his analysis and interpretation of the effect as the skipping orbit counterpart of the Koch–Kuo skimming orbit theory[5] leaves much to be desired. This serves to emphasize that the effect is very much a quantum-mechanical affair. The dominant resonances are due to transitions between states with small quantum numbers n, and the resonance condition is not immediately related to the skipping frequency, but instead occurs when the microwave frequency ω equals the quantum mechanical difference or beat frequency $\omega_n-\omega_m$.

In the following section, we give an elementary derivation of the Prange–Nee surface states. This "back-of-an-envelope" approach emphasizes essential physical aspects, without involving the reader in Hamiltonians, choice of gauge questions, expansions, and complicated mathematical functions. Section III gives some experimental details with particular emphasis on the matter of surface preparation. Section IV presents a detailed numerical calculation of the impedance oscillation spectrum and establishes how to obtain accurate values of Fermi-surface parameters from the experimental curves. Section V deals with the results of the present investigation and relevant dis-

[1] T. W. Nee and R. E. Prange, Phys. Letters **25A**, 582 (1967).
[2] R. E. Prange and T. W. Nee, Phys. Rev. **168**, 779 (1968).
[3] M. S. Khaikin, Zh. Eksperim. i Teor. Fiz. **39**, 212 (1960) [English transl.: Soviet Phys.—JETP **12**, 152 (1961)].
[4] J. F. Koch and A. F. Kip, *Low Temperature Physics LT9* (Plenum Press, Inc., New York, 1965), p. 818–822.
[5] J. F. Koch and C. C. Kuo, Phys. Rev. **143**, 470 (1966).
[6] M. S. Khaikin, Zh. Eksperim. i Teor. Fiz. Pis'ma v Redaktsiyu **4**, 164 (1966) [English transl.: Soviet Phys.—JETP Letters **4**, 113 (1966)].
[7] J. F. Koch, *Solid State Physics*, (Gordon and Breach, Science Publishers Inc., New York, 1968), Vol. I.
[8] R. Herrmann, Phys. Status Solidi **21**, 703 (1967).
[9] T. W. Nee, J. F. Koch, and R. E. Prange, Phys. Rev. **174**, 758 (1968).
[10] H. J. Fishbeck and J. Mertsching, Phys. Status Solidi **27**, 345 (1968). (In this work the conclusion that dR/dH zeros represent the resonance criterion is incorrect.)

cussion. In Sec. VI we conclude with some remarks on aspects of future work in Bi.

II. SURFACE QUANTUM STATES: A "MINIMAL THEORY"

While we refer the serious reader to the detailed theoretical discussion by Prange and Nee,[2] and sketch here only a "back-of-an-envelope" approach to surface quantum states to provide the necessary background to the present experiments. This is decidedly a minimal account that leaves some details unanswered.

As in Fig. 1, we consider an electron moving along the surface of the metal by periodic specular reflection. This skipping trajectory describes a state in which the electron is bound to the surface region. It is trapped in a potential well formed on one side by the metal-vacuum interface potential, on the other by the magnetic field induced potential that confines it to the classical turning point of the circular motion. In the weak magnetic fields (a few Oe) where the experiments are done, the cyclotron radius R_c is typically on the order of 1 cm. The microwave fields penetrate to a characteristic skin depth on the order of 10^{-5} cm. With these considerations in mind, we see that out of the entire spectrum of possible colliding orbits only those, for which the electrons are moving essentially parallel to the surface (i.e., very shallow trajectories), will make an important contribution to the surface currents. Their duty-cycle is much larger than that of electrons which move deeply into the metal between successive collisions. Together with the fact that the microwave photon energy $\hbar\omega$ is very mcuh less than the Fermi energy E_F (and transitions, consequently, take place only in the immediate vicinity of the Fermi surface), this implies that we may restrict our attention to electrons moving along the surface with velocity v_x approximately equal to v_F, the Fermi velocity. Moreover, we may take v_x to be essentially constant throughout each cycle of the skipping motion and consequently the electrons experience a nearly constant Lorentz force

$$F=ev_FH \tag{1}$$

impelling them toward the surface. The corresponding potential may be taken as

$$V(z)=(ev_FH)z. \tag{2}$$

We are therefore concerned with a particle confined to a triangular potential well, rattling around between the impenetrable potential barrier at the surface and the classical turning point of its circular motion. The possible energy states ϵ_n (as measured from the Fermi energy E_F) are described in terms of quantum-mechanically allowed values of the maximal depth of penetration z_n as

$$\epsilon_n=(ev_FH)z_n. \tag{3}$$

For the periodic z-directed motion, we require

$$\oint p_z dz=2\int_0^{z_n} p_F\frac{\sqrt{2}(z_n-z)^{1/2}}{R^{1/2}}dz=(n-\tfrac{1}{4})h, \tag{4}$$

where p_z has been expressed in terms of the Fermi momentum p_F and appropriate geometrical factors. R represents the radius of the skipping trajectory. The phase factor of $\frac{1}{4}$ is chosen appropriately for the case of a single linear turning point of the motion. Evaluating the integral and solving for z_n we obtain

$$\begin{aligned} z_n&=\left|\frac{3}{4\sqrt{2}}(n-\tfrac{1}{4})\frac{hR^{1/2}}{p_F}\right|^{2/3}\\ &=|\tfrac{3}{4}\sqrt{\pi}(n-\tfrac{1}{4})|^{2/3}\left(\frac{h}{e}\right)^{1/3}\frac{1}{H^{1/3}K^{1/3}}, \end{aligned} \tag{5}$$

where in the final step we have chosen to relate both the cyclotron radius R and Fermi momentum p_F, to the radius of curvature K of the Fermi surface in k space (i.e., $R=\hbar K/eH$, $P_F=\hbar K$). Consequently, the energy-level scheme for the surface states appears as

$$\epsilon_n=|\tfrac{3}{4}\sqrt{\pi}(n-\tfrac{1}{4})|^{2/3}(e^2h)^{1/3}H^{2/3}\left(\frac{v_F}{K^{1/3}}\right). \tag{6}$$

In the adjoining figure we have sketched a few of the lowest-energy levels and indicated possible microwave transitions between them. The spectrum of surface impedance oscillations is expected to consist of several series of peaks each characterized by a given ground state and going to successively higher states.

Since we have made use of the Bohr–Sommerfeld rule in our derivation and short-circuited more exact mathematics, the energy-level scheme in Eq. (6) differs from the expression derived by Prange and Nee[2] by about 1% for the lowest-lying states. The factor $|\frac{3}{4}\sqrt{\pi}(n-\frac{1}{4})|^{2/3}$ ought to be replaced by $\zeta_n/(2\sqrt{\pi})^{2/3}$, where ζ_n is the nth root of the Airy function. For the

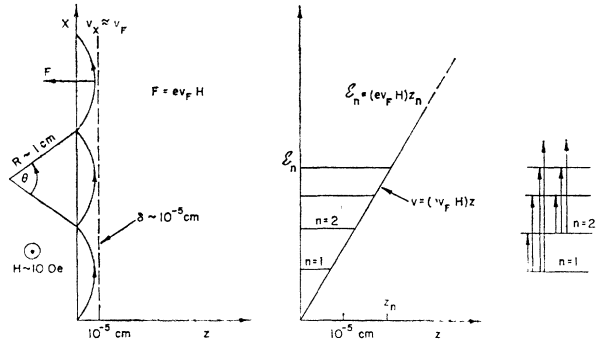

FIG. 1. Electrons skipping along the surface of the metal correspond to quantum-mechanical states in the triangular potential well. Allowed transitions give rise to series of spectral lines in the microwave surface impedance. Each series is characterized by a given lower level and transitions going to successively higher states.

comparison of calculated and observed peak positions, we shall take advantage of this more accurate formulation, using the ζ_n in later formulas.

We conclude the present discussion by calling the readers attention to an amusing alternative interpretation of the quantization of orbit depths z_n [Eq. (5)]. The area swept out in each cycle of the skipping motion is readily shown to be $(4\sqrt{2}/3)R^{1/2}z_n^{3/2}$, and consequently the flux enclosed between the surface and the classical trajectory will be quantized as

$$\Phi_n=(4\sqrt{2}/3)R^{1/2}z_n^{3/2}H=(n-\tfrac{1}{4})h/e. \quad (7)$$

We may contrast this result with the elementary discussion of Landau levels, which gives the flux enclosed by electrons in allowed cyclotron orbits as $(n-\frac{1}{2})h/e$.

III. EXPERIMENTAL ASPECTS

The experiments are carried out using a standard microwave reflection spectrometer. The sample forms the end wall of a cylindrical cavity resonator operated in the TE_{111} mode. The earth's magnetic field is cancelled to better than 0.05 Oe by a set of three mutually perpendicular pairs of Helmholtz coils. A fourth set of coils provides the experimental field. This last field is carefully calibrated from the observation of electron spin resonance of a diphenyl picryl hydrazyl sample in an NMR apparatus to an accuracy better than $\pm 0.3\%$.

Single crystals of the major symmetry planes of Bi, and several orientations in which the long axis of the electron ellipsoid was parallel to the surface, were prepared by spark-cutting from Cominco 69 grade ingots. Because the long axis of the electron ellipsoid is tilted out of the trigonal (C_3) plane by approximately 6.5°, we had to take great care in orienting and cutting specimens. The sense of tilt was determined by studying the variation of the cyclotron mass in the binary (C_2) plane as the magnetic field was rotated about the bisectrix (C_1) axis. The sign of the tilt was referred to the triangular etch pits on the side of the binary sample. The sense of tilt could then be obtained unambiguously for other samples with reference to the triangular etch pits, as has also been noted recently by Brown *et al.*[11]

After spark-cutting, the sample surface was lapped gently on a Teflon cloth saturated with a solution of nitric acid, glacial acetic acid, and water (6:6:1). The final step in the surface preparation was electropolishing in a saturated solution of potassium iodide and concentrated HCl (49:1). The polishing procedure was to use high current densities ($\sim$ several A/cm^2) for short periods. The deatils were dictated by the formation of a brownish film on the surface of the sample. This film should be produced quickly and the current removed precisely when the surface is completely covered. This technique worked well for all orientations other than the trigonal (C_3) plane. The C_3 plane was polished chemically by immersion in the lapping solution, while it was being stirred. This method generally proved satisfactory for small specimens and gave some of the best data in the present experiments.

A third method of sample surface preparation, was to grow samples from the melt against lightly carbon-coated polished quartz slides. The surfaces, when removed from the mold, appeared smooth and shiny but had a considerable amount of small carbon particles imbedded in it. These samples have really inferior signals, and improved when they were electropolished to remove the surface layer. Because of the difficulties in accurately seeding such as-grown samples, we reverted to the technique of cutting, lapping, and polishing for most of the samples.

IV. CALCULATIONS OF THE IMPEDANCE SPECTRUM

To make an accurate evaluation of the Fermi-surface parameters from the experimental data requires an exacting analysis and interpretation of the line shape of the resonant impedance variations. The original supposition that dR/dH peaks approximately correspond to the resonance condition[1] has since been confirmed and supplanted by a detailed calculation of the impedance due to Nee, Koch, and Prange (NKP).[9] Such calculations have been based on what the authors refer to as the cylindrical approximation, where all electrons contributing to the resonance are assigned constant values of Fermi-surface parameters, relaxation times and other ingredients of the calculation. This magnanimous approximation to the real Fermi surface, it has been suspected, accounts in large part for the remaining discrepancies apparent in a comparison of theoretical and experimental resonance curves. Below we shall show that following along the lines suggested by Koch,[12] it is possible to calculate the spectrum including the k_y broadening for certain restricted Fermi-surface geometries.

The ellipsoidal Fermi-surface geometry of Bi is ideally suited to this calculation and has allowed us to make a calculation that compares favorably with the experimental curve. Fitting of theory to experiment allows us to evaluate accurately the resonance field values from experimental curves. This is a necessary part of evaluating the data. Depending on the values of relaxation time, skin depth, and Fermi-surface geometry, the resonance field can easily differ by 5% or more from the observed peak position for the case of the 1-2 transition.

Following the work in Refs. 2 and 9. we write the

[11] R. D. Brown, R. L. Hartman, and S. H. Koenig, Phys. Rev. **172**, 598 (1968).

[12] J. F. Koch, Physik Kondensiertan Materie **9**, 146 (1969).

expression for the impedance derivative dZ/dH as

$$\frac{dZ}{dH}=\text{const}(i-\sqrt{3})\frac{d}{dH}\int dk_y v_x(k_y) \times\sum_{m,n}\frac{\alpha_{mn}^2(k_y,H,\delta)}{\omega-\omega_{mn}(H,k_y)+i\Gamma_{mn}(k_y,H)}. \quad (8)$$

The geometry here is such that H is in the y direction and parallel to the sample surface. The rf current is in the x direction, which is also chosen to be one of the principle directions of the impedance tensor. α_{mn} is the matrix element of the normalized electric field $E(z)/E(0)$ taken between surface-state wave functions ϕ_n and ϕ_m. The matrix elements depend on the range of penetration of the electric field, i.e., on the skin depth δ. They are dependent on magnetic field and position on the Fermi surface, through the dependence of the wave functions on H and the local radius of curvature $K_\perp$ at the Fermi surface. ω_{mn} is the difference frequency $\epsilon_m-\epsilon_n/\hbar$ of a pair of surface states, and obviously depends on both H and k_y.

The finite lifetime of an electron in a surface-state trajectory is reflected in an energy-level frequency width Γ_n, which may depend on both k_y and H. The quantity Γ_{mn} is the mean width $\frac{1}{2}(\Gamma_m+\Gamma_n)$ for a pair of states. The doubly infinite sum over m and n adds up the contribution to the impedance of all pairs of surface states at a specific place on the Fermi surface, whose coordinate along the magnetic field direction is k_y. The velocity $v_x(k_y)$ is the component of the Fermi velocity in the direction of the applied electric field. Finally and most importantly, the k_y integral sums the resonance signals of electrons everywhere on a narrow strip on the Fermi surface. This effective zone is centered symmetrically about the line defined by $v_z=0$, has an angular width of a few degrees in Bi, and contains

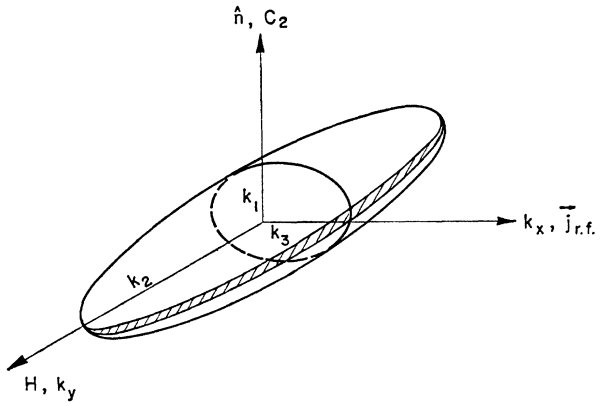

FIG. 2. Skipping electrons repeatedly traverse a zone centered about the line $v_z=0$ and with an angular width of a few degrees. For data taken with the magnetic field along the ellipsoid major axis in the binary plane sample, the skipping zone is as indicated n the figure.

electron states for which the direction of v_x is such that they are bent toward the surface.

In Fig. 2, we have sketched the zone containing the skipping electron states for an ellipsoidal sheet of Fermi surface aligned with the sample surface. We expect that the observed resonance signal will be dominated by electrons on the zone for which $\omega_{mn}(k_y)$ has a stationary value, but recognize that the linewidth and shape of the resonance will be decisively influenced by neighboring electron states. The problem is to calculate the resonance signals taking this k_y broadening into account, and thus to relate the resulting resonance curve to the parameters associated with the extremal electron states.

We next express the impedance formula in terms of a suitably normalized field coordinate h defined by

$$h=\frac{e}{\hbar}(v_x^3/2K\omega^3)^{1/2}H=\gamma H, \quad (9)$$

such that the resonant field values are given by

$$h_{mn}=(\zeta_m-\zeta_n)^{-3/2}. \quad (10)$$

With reference to NKP, we see that the matrix elements α_{mn} that appear in the impedance formula are functions of the normalized field h and depend on a single parameter β given by

$$\beta=(v_x/2K\omega)^{1/2}(1/\delta). \quad (11)$$

As a final step, we interchange the differentiation d/dH with the k_y integration, and express the derivative in terms of the normalized field to obtain the impedance formula as

$$\frac{dZ}{dH}=\text{const}\int dk_y v_x\gamma\frac{d}{dh} \times\sum_{m,n}\frac{(i-\sqrt{3})\alpha_{mn}^2(\beta,h)}{1-h^{2/3}(\zeta_m-\zeta_n)+(i/\omega\tau)}. \quad (12)$$

The level frequency width Γ_n has been taken as $1/\tau$, the reciprocal of the relaxation time due to bulk scattering events. This is equivalent to treating the surface as adequately smooth, so that the lack of specular scattering (which is expected to be field dependent) makes no significant contribution to the level width. A further approximation essential to our calculation is to take the relaxation time τ as independent of k_y and equal to its value for the group of electrons with extremal ω_{mn}. The quantities h, v_x, γ, as well as the parameter β, are to be considered functions of k_y.

The factor $d/dh\sum(\ )$ that appears in the integrand is obviously a function of h and depends on two parameters, namely, β and $\omega\tau$. It represents the resonance spectrum of a single cylindrical section as discussed in NKP. We have available to us a library of such computer generated curves for physically realistic values of

β and $\omega\tau$. Let us call these curves $F\ (h=\gamma H;\beta,\omega\tau)$ and suppose the values of β and $\omega\tau$ to be constant along a zone such as that of Fig. 2. If we imagine this zone to be subdivided into a number of strips with length Δk_{yn}, then for every strip the resonance curve in normalized field h [i.e., $F(h;\beta,\omega\tau)$] would be identical. Expressed in terms of the actual field H, the curve would retain its form but have a different horizontal field scale $H=h/\gamma(k_{yn})$. The procedure for computing the k_y integral is completely straightforward now. We start with a library curve, choose the desired variation of v_x and γ with k_y, and compute the sum of curves each of which has had its field scale adjusted according to $\gamma(k_y)$ and has an amplitude proportional to $\Delta k_{yn}v_x(k_{yn})\gamma(k_{yn})$. The sum

$$\frac{dZ}{dH}=\text{const}\sum_n \Delta k_{yn}v_x(k_{yn})\gamma(k_{yn})F(\gamma(k_{yn})H;\beta;\omega\tau) \quad (13)$$

evaluated over a sufficiently narrow set of strips, gives the impedance derivative for the actual Fermi surface.

This deceptively simple evaluation of the k_y integral is possible only when both β and τ can be considered constant along the entire strip. From the definition of β, we see that it is proportional to $(v_x/K_1)^{1/2}$, a quantity which for the case of a quadratic dispersion law is indeed constant along a zone such as that in Fig. 2. A constant relaxation time, equal to its value at the center of the zone, is more difficult to justify. However, because essential contributions to the resonance come from Δk_y strips in the vicinity of the ω_{nm} extremum, it should not be a bad approximation.

We now turn to a critical examination and calculation of a single resonance curve in Bi. The data of Fig. 3 show oscillations in the surface resistance derivative observed with the magnetic field along the major axis of the electron ellipsoid for a binary plane specimen. The rf current is arranged to flow along the trigonal axis,

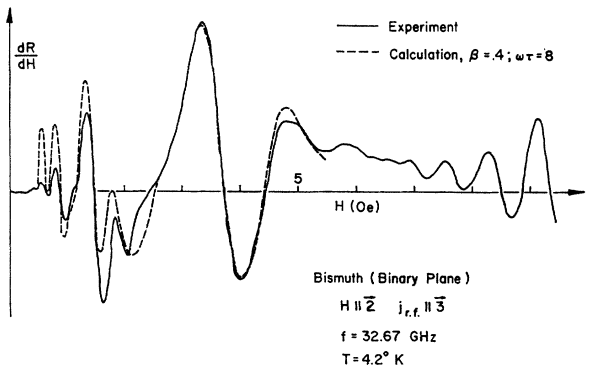

FIG. 3. Comparison of the experimentally observed dR/dH curve in the Bi binary plane and a calculated curve ($\omega\tau=8$; $\beta=0.4$) that includes the k_y broadening. The calculation allows us to accurately identify the resonance field from the experimental data.

which is a principal axis of the impedance tensor. The frequency is 32.67 GHz and the sample is at 4.2°K. The spectrum of oscillations below 6 Oe is due to resonant transitions between surface states, while at higher fields there appear Azbél-Kaner cyclotron resonance peaks.

To calculate the spectrum, we have examined a set of library curves with different values of β and $\omega\tau$. Of these, the $\beta=0.4$; $\omega\tau=8$ curve provides a good starting point for the k_y calculation. The geometry is such that electrons in surface states move about on the zone indicated in Fig. 2. The parameter β is constant along the zone if we take the Fermi surface as ellipsoidal in shape and assume a parabolic dispersion law (the EP model). The velocity v_x varies along the zone as

$$v_x(k_y)=(\hbar k_3/m_3)(1-k_y^2/k_2^2)^{1/2}, \quad (14)$$

where k_1, k_2, k_3 are the semimajor and minor axes of the ellipsoid (Fig. 2), and m_3 is the appropriate band-mass parameter. The radius of curvature in the plane perpendicular to the magnetic field is given by

$$K_\perp=(k_1^2/k_3)(1-k_y^2/k_2^2)^{1/2}. \quad (15)$$

The quantity $v_x/K_\perp$ is constant along the zone, and this justifies the calculational procedure outlined above.

The variation of the field scaling parameter $\gamma(k_y)$ is calculated in the same way. We substitute the values of v_x and $K_\perp$ to find

$$\gamma(k_y)=\gamma(0)(1-k_y^2/k_2^2)^{1/2}, \quad (16)$$

where $\gamma(0)$ represents the field scaling factor for the center of the zone. $\gamma(k_y)$ has its maximum value for $k_y=0$ and decreases only slowly in the neighborhood of this region. The resonance signals of electrons along the zone fall at increasingly higher actual field H as we move out from the center.

With the information on $v_x(k_y)$, $\gamma(k_y)$ at hand, we are ready to take the library curve $\beta=0.4$ and $\omega\tau=8$ and calculate the k_y integral. We choose $\gamma(0)$ such as to overlap the resonance peaks at 3.34 Oe precisely, and adjust the amplitude to match the experimental trace. The two curves are then superposed (Fig. 3) to show to what extent we can get theory and experiment to agree. In achieving this fit we have actually examined curves for which β had values 0.35, 0.4 and 0.45, and $\omega\tau$ ranged in integral steps from 6 to 10. The values $\beta=0.4$ and $\omega\tau=8$ gave the best fit and are expected to be accurate to ±0.05 and ±0.5 for the two quantities, respectively. To try harder at achieving a perfect fit would be meaningless, because we suspect that another weak signal, due to the other two ellipsoids of the Fermi surface, is interfering in the experimental trace and that possibly there is some baseline effect present in the experiment. The amplitude difference of the peaks at the very lowest fields is likely to be a real discrepancy. For reasons as yet unknown, the experimental trace

always shows the low-field resonances to damp out more quickly than the calculation would predict.

A critical comparison of the k_y broadened curve and the library curve, that was the starting point of the calculation, convinces us that the calculation of the k_y integral is important in more than one way. There is a small increase in the width of the peaks, a notable decrease in the amplitude of the low-field peaks relative to high-field peaks due to interference effects, and most importantly a shift in peak positions by several percent. This is of course crucial to an accurate determination of the Fermi-surface parameters from the experimental data. Our work with the calculations has shown that the major resonance peak due to the $n=1$ to $m=2$ transition (at 3.34 Oe in Fig. 3) moves with changes in $\omega\tau$, β, and the nature of the anisotropy of $\gamma(k_y)$. Because many of our data appear similar to those of the test case that we have fit and discussed here, we take our clues from this example. In terms of numbers, the 1-2 peak in the calculated spectrum occurs at $h=0.427$, while the resonance condition gives $h_{21}=0.432$. Thus the resonance field for the center of the zone will be taken proportionately higher than the experimentally determined peak field. Since $\gamma(k_y)$ is identical for all the samples used to determine v_F on the central section of the Bi ellipsoid, and since β and $\omega\tau$ do not vary widely, we feel safe in assuming that resonance fields determined from the experiments are well within the estimated limits of error.

In the fitting procedure, we have considered both β and $\omega\tau$ as parameters, to be adjusted and determined from the comparison of theory and experiment. This is fine as far as $\omega\tau$ is concerned, but the value of β depends on known Fermi-surface parameters and the skin depth δ. Since there exist measurements of the anomalous skin effect (ASE) resistance in Bi that could be interpreted in terms of a skin depth, β should not be considered a disposable parameter. If, following Smith,[13] we take the ASE resistance value (for the binary plane with current flowing along trigonal axis) as 0.075 Ω at 23.5 GHz, we can derive a skin depth from the relation $R=8\pi/3\sqrt{3}(\omega/c^2)\delta$. We find $\delta=1.05\times10^{-4}$ cm. Scaled to the present frequency of 32.67 GHz, this becomes 0.94×10^{-4} cm. Using the Fermi-surface dimensions in Eq. (17), and taking the velocity value derived in the experiments (Sec. V), we arrive at $\beta=0.24$. A calculation with this value of β proved very different from the experimental curve, so that we found it necessary to revert to an adjustable β. We are disturbed about this discrepancy. Using $\beta=0.4$ gives a skin depth and ASE resistance a full 40% smaller than that measured by Smith. Aubrey's[14] ASE measurements at 9 GHz disagree with Smith's by about 20%, but in the wrong direction to resolve the present discrepancy.

[13] G. E. Smith, Phys. Rev. **115**, 1561 (1959).
[14] J. E. Aubrey, J. Phys. Chem. Solids **19**, 321 (1961).

Another source of concern is the relatively low value of $\omega\tau$ that we derive. Judging by the 15 cyclotron harmonics that are observed in the specimen, we had expected a value of $\omega\tau$ close to 15. It is possible that there is anisotropy of τ over the Fermi surface, and that the value of τ is smaller at the zone responsible for the surface states. More likely however, the small $\omega\tau$ reflects increased scattering in the surface region because of larger phonon amplitudes and possibly because of a greater concentration of diffused impurities close to the surface. There may also be a small contribution of diffuse surface scattering to account for the disparity of cyclotron and surface-state relaxation times.

V. RESULTS AND DISCUSSION

We preface this section with the necessary facts on the Bi Fermi-surface geometry, as well as some available information on the band structure. The Bi crystal structure is rhombohedral, but alternatively may be derived from a simple cubic lattice in which one of the body diagonals (the [111] axis of the cube) is elongated somewhat to achieve the appropriate distortion. This special body diagonal retains the threefold rotation symmetry of the cubic lattice and becomes the trigonal direction C_3 of the Bi lattice. The binary C_2 and bisectrix C_1 axes are two mutually perpendicular directions contained in the trigonal plane as indicated in Fig. 4.

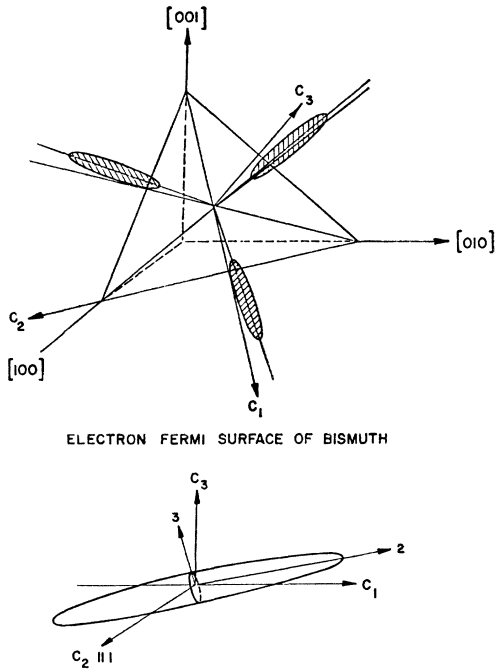

FIG. 4. The Bi electron Fermi-surface geometry and relevant directions. The ellipsoids are tilted out trigonal (C_3) plane by 6°20′. The principal axes of the ellipsoid are denoted as **1**, **2**, **3**, and are arranged relative to the crystal axes (C_1, C_2, and C_3) as shown in the lower half of the figure.

Bi is a compensated metal with a single-hole Fermi surface and three electron surfaces. The angular variation and symmetry of the surface-state data in this metal are characteristic of the electron surfaces with no evidence for any signal due to the holes. For this reason, we restrict the discussion to the electron surfaces. These are in the form of elongated ellipsoids arranged with their major axes nearly along C_1 as sketched in the figure. They are tilted out of the trigonal plane toward the C_3 axis by 6°20′. We judge the recent de Haas-van Alphen (dHvA) effect studies of Bhargava[15] to provide the most definitive and up to date geometrical information on the electron ellipsoids. For one, Bhargava's data establish the ellipsoidal shape of the electron surfaces, and secondly from his measured cross-sectional areas we can derive the dimensions of the major and minor axes of the ellipsoid. Expressed in terms of the principal axis system (**1,2,3**) of the ellipsoid these are

$$\begin{aligned} k_1&=5.16\times10^5\ \text{cm}^{-1}\\ k_2&=84.4\times10^5\ \text{cm}^{-1}\\ k_3&=6.78\times10^5\ \text{cm}^{-1}. \end{aligned} \tag{17}$$

So much of the numerical interpretation of our data depends on accurate knowledge of the geometry and dimensions of the electron surfaces, that much of it would need considerable modification and adjustment if there were serious errors in the stated dimensions, or if the shape were not ellipsoidal. In discussing results and estimating errors, we will deal with the geometrical data on the ellipsoid geometry as the "truth." We take solace from the fact that most of our analysis involves only values of the minor axes k_1 and k_3. The axis k_1 has been measured independently by cyclotron cutoff[16] and ultrasonic attentuation[17] to yield 5.2×10^5 cm^{-1}, i.e., it agrees within 1% with Bhargava's value. In turn the dHvA measurements give the area of the 1,3 cross section very accurately, so that k_3 is also well determined. We are alarmed, however, at the wide discrepancy in numbers quoted for k_2. Korolyuk[17] finds $k_2=72\times10^5$ cm^{-1}, while according to Bhargava's data this dimension is 84.4×10^5 cm^{-1}.

While there is relatively good agreement on the basic geometry of the electron surfaces, the band structure is another matter. There are three different proposed descriptions of the relation of energy and momentum; the ellipsoid-parabolic (EP) model,[18] the ellipsoidal nonparabolic (ENP)[19] model, and the nonellipsoidal-nonparabolic (NENP)[20] model. Since the velocity values derived in this experiment depend solely on geometrical factors, we need not really concern ourselves with details of band descriptions. Only for purposes of comparison do we want to become involved with band-mass parameters. For this purpose, we choose the EP description, where the electron energy is given by

$$E=\tfrac{1}{2}\hbar^2\left|k_1^2/m_1+k_2^2/m_2+k_3^2/m_3\right|, \tag{18}$$

with $m_{1,2,3}$ as the mass parameters. Using what we consider the best available data on cyclotron effective masses in Bi[21] and the standard relation between cyclotron and band masses, one obtains

$$\begin{aligned} m_1&=0.0058m_0,\\ m_2&=1.28m_0,\\ m_3&=0.011m_0, \end{aligned} \tag{19}$$

where m_0 is the free-electron mass. We will later compare these values with some that we can derive from our velocity measurements.

Below, we consider in detail each of the different aspects of our experiments on surface quantum states in Bi.

A. dR/dH Oscillation Spectrum

We start with some qualitative observations on the inevitable "typical" data shown in Fig. 5. The magnetic field is arranged to lie parallel to the sample surface and along the major axis of one of the electron ellipsoids. The sample surface is such that the surface normal $\hat{n}$ makes an angle of 56° with principal axis 3 of the ellipsoid. The polarization of the rf currents is chosen to avoid contributions from the remaining two

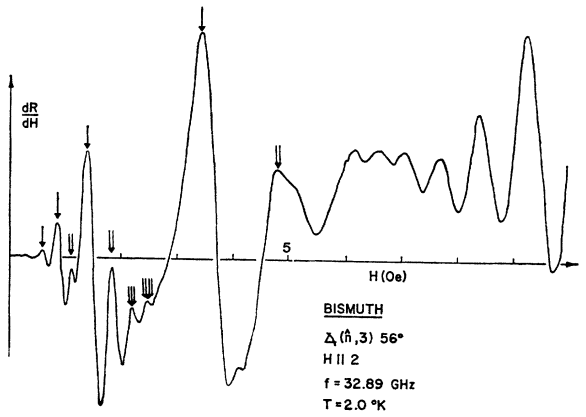

FIG. 5. *dR/dH* oscillation spectrum in Bi sample No. 7. The series of resonance transitions starting with the $n=1$ ground state and going to $m=2,3,\cdots$, etc, is marked with single arrows. Double arrows represent the corresponding series with $n=2$, and so on. Oscillations above 5 Oe are due to Azbél-Kaner cyclotron resonance with a mass of $(0.0077\pm0.0002)m_0$.

[15] R. N. Bhargava, Phys. Rev. **156**, 785 (1967).
[16] M. S. Khaikin and V. S. Edelman, Zh. Eksperim i Teor. Fiz. **47**, 878 (1964) [English transl.: Soviet Phys.—JETP **20**, 587 (1965)].
[17] A. P. Korolyuk, Zh. Eksperim. i Teor. Fiz. **49**, 1009 (1965) [English transl.: Soviet Phys.—JETP **22**, 701 (1966)].
[18] D. Shoenberg, Proc. Roy. Soc. (London) **A170**, 341 (1939).
[19] B. Lax, J. G. Havroides, H. J. Zeiger, and R. J. Keyes, Phys. Rev. Letters **5**, 241 (1960).
[20] M. H. Cohen, Phys. Rev. **121**, 387 (1961).
[21] V. S. Edelman and M. S. Khaikin, Zh. Eksperim. i Teor. Fiz. **49**, 107 (1965) [English transl.: Soviet Phys.—JETP **22**, 77 (1966)].

ellipsoids, so that the observed dR/dH oscillations are due to a single sheet of the electron surface.

The spectrum of dR/dH peaks at fields below 6 Oe represent microwave resonant transitions between surface quantum states, while the oscillatory variations at higher fields are due to Azbél-Kaner cyclotron resonance in this specimen. The cyclotron resonance signal serves to judge the quality of the specimen and also provides an independent measurement of the cyclotron effective mass. The series of peaks starting at $H=3.44$ Oe and marked with single arrows, dominates the low-field pattern of resonances. Even without the benefit of detailed calculations, we would ascribe the four peaks of this series to transitions from the ground state $n=1$ trajectory to successively higher states ($m=2$, 3, 4, and 5) as the field is decreased. This is because the $n=1$ trajectory is most strongly exposed to the rf fields in the skin layer. Peaks starting at 4.80 Oe, and identified with double arrows, represent transitions from $n=2$ to successively $m=3$, 4, 5. The fundamentals of the triple arrow and higher series are obscured by cyclotron resonance, while second peaks of these series can still be resolved and have been marked accordingly.

The pattern of oscillations in Fig. 5 is characteristic of surface state resonances and serves to identify the effect. An examination of the relative positions of the resonance peaks provides a quick check on the energy-level scheme for the surface states. In Table I, we give a comparison of calculated and experimentally observed resonance fields in terms of the normalized field coordinate h. The experimental resonance fields are expressed relative to the peak at 3.44 Oe, which we identify as the transition $\epsilon_2-\epsilon_1=\hbar\omega$, and which is expected to occur at $h=0.432$. The lack of perfect agreement arises partly because of experimental uncertainty in the determination of the resonance peaks, but also because the experimental peaks do not exactly coincide with the resonances. This is apparent from the calculations of Sec. IV.

TABLE I. Normalized resonance fields h_{nm}.

n	m	h_{nm}(theory)	$(dR/dH)_{max}$ fields (Fig. 5) normalized s.t. 3.44 Oe=0.432
1	2	0.432	0.432
	3	0.176	0.172
	4	0.107	0.103
	5	0.075	0.071
2	3	0.583	0.603
	4	0.226	0.228
	5	0.132	0.132
3	4	0.702	not resolved
	5	0.265	0.275

B. Calculation of Peak Positions from Band-Structure Parameters

The established Fermi-surface parameters in Bi provide us with the means to make an even more demanding check on the theory of the surface states by actually calculating the theoretically expected resonance field H_{12}. Previous comparisons of theory and experiment[1,9] had to content themselves with showing that for reasonable choices of Fermi-surface parameters one could get agreement with observed resonance fields. For the case of Bi, we can make a more critical comparison.

We take, for example, data observed in the binary and "almost trigonal" plane samples, listed, respectively, as samples No. 8 and No. 1 in the Table II of the next section. With the field parallel to the major axis of the ellipsoid in these two planes, we find H_{12} to be 3.39 and 3.52 Oe for the two planes, respectively, and at a microwave frequency of 32.77 GHz. These field values represent, as we have discussed in the section on line shape calculation, the resonance field for the electrons at the central cross section of the electron ellipsoid.

The field values measured in the experiments are to be compared with values calculated from the theoretical expression for the energy-level scheme [Eq. (6)]. For resonant transitions between the $n=1$ and $m=2$ surface states we require that the microwave photon energy $\hbar\omega$ be equal to the energy-level separation $\epsilon_2-\epsilon_1$. Solving for the magnetic field value where this is satisfied, we obtain

$$H_{12}=0.432(\hbar/e)\omega^{3/2}(2K/v^3)^{1/2}. \quad (20)$$

With the field along the major axis of the ellipse for the "almost trigonal" sample, the electron repeatedly traverses a zone with local radius of curvature $K=k_3^2/k_1=8.9\times10^5$ cm^{-1}. The velocity at this point is given by the EP description of the band structure as $v=\hbar k_1/m_1=1.0\times10^8$ cm/sec. Substituting into the equation for H_{12}, we calculate a resonance field of 3.4 Oe at a microwave frequency of 32.77 GHz. This is to be compared with the experimental value of 3.52 Oe $\pm2\%$. We obtain satisfactory agreement for this orientation in spite of the large uncertainties associated with the established band parameters.

For the binary-plane data, we proceed as above to evaluate K and v and calculate a resonance field H_{12}

TABLE II. Resonance fields H_{12} and Fermi velocities.

Sample No.	Position of surface normal n $\sphericalangle(n,3)$	Position of skipping zone $\sphericalangle$(zone, 1)	H_{12}Oe$\pm2\%$ $f=32.77$ GHz	v_F (experiment) $\pm1.5\%$
1	0°	0°	3.52	10.1×10^7 cm/sec
2	5°	8°	3.53	10.0
3	10°	17°	3.40	10.2
4	22°	35°	3.45	9.7
5	36°	52°	3.39	9.2
6	44°	60°	3.48	8.6
7	56°	70°	3.49	8.2
8	90°	90°	3.39	7.8

of 4.0 Oe. The experiment gives 3.39 Oe, with an error not exceeding $\pm 2\%$. This discrepancy of calculated and experimental values for the binary plane, we suspect, is due to an incorrect value of m_3.

This examination and comparison of calculated and experimental values of resonance fields leads us to conclude that the theoretical description of surface states is essentially correct in its numerical aspects. These studies in Bi are the first to provide an absolute confirmation of the Prange–Nee energy-level scheme for the surface states. More recent work in Cu [12] and Ag,[22] where it is also possible to compare theory and experiment in absolute terms, give equally satisfactory agreement.

C. Determination of Fermi Velocities at Individual Points

Convinced by the reasonable agreement of calculated and observed peak positions that the formulation of the surface-state problem is essentially correct, we now work the experiment backwards. From the experimentally determined peak positions, in conjunction with the line shape computations, we measure the resonance field H_{12} in a series of eight different samples. These are cut so that the electron ellipsoid always lies in the sample plane, but the skipping zone appears at eight different places. The reader may imagine that we start with the binary plane sample and rotate the surface normal $\hat{n}$ of Fig. 2 about the k_2 axis to eight positions in a quadrant of the elliptical cross section. The zone moves in such a way that the Fermi-velocity vector is perpendicular to $\hat{n}$. This position is determined from the measured angle of rotation of $\hat{n}$ away from the binary axis and the known shape of the ellipsoidal surface. For each of these points, we then calculate the appropriate radius of curvature K, and from the measured resonance field H_{12} and microwave frequency ω obtain the Fermi velocity v_F at the position of the zone. We emphasize, that in evaluating Fermi velocities in this way, we have made use solely of the geometry of the Fermi surface, without involving band-mass parameters or any assumptions about the nature of the dispersion relation $E(k)$.

In Table II, we give the H_{12} values for each of the eight samples, together with the measured angle of the surface normal $\hat{n}$ relative to the binary axis. The values H_{12} have been corrected from the measured peak positions, as suggested by the detailed calculation and fitting of the binary plane spectrum, and therefore represent the resonance field for the $k_y=0$ electrons on the zone. In many cases, the values H_{12} are obtained by averaging over several specimens of a given orientation, over runs at somewhat different frequencies, and using different surface polishes. The possible error in H_{12} is at most $\pm 2\%$ due to uncertainties in locating peaks accurately, possible minor discrepancies in the fitting scheme, inaccuracies in the cutting and aligning of the sample, errors in the absolute calibration of the field, etc. The uncertainty in the calculated velocities is more difficult to ascertain, since it depends so much on the input of information on the Fermi-surface geometry. If we consider the geometrical data from the dHvA effect as sufficiently accurate, the possible error in the velocities should not exceed $\pm 1.5\%$. One other possibility of error lies in our assumption that the entire cycle of the skipping motion may be approximated as a small portion of a circular orbit with a unique radius of curvature $K_\perp$ on the Fermi surface. In Bi, the skipping electron moves through an angular range of several degrees, and velocity values are to be considered as averaged over a few degrees of the elliptical section.

The velocity values derived from our experiments are plotted in Fig. 6 at each of the points on the elliptical cross section where it has been measured. The velocities are found to range from a maximum of 10.1×10^7 cm/sec in the binary direction to a minimum value of 7.8×10^7 cm/sec along the trigonal direction. There exist some other measurements of velocities at individual points on the Bi surface, with which the present data can be

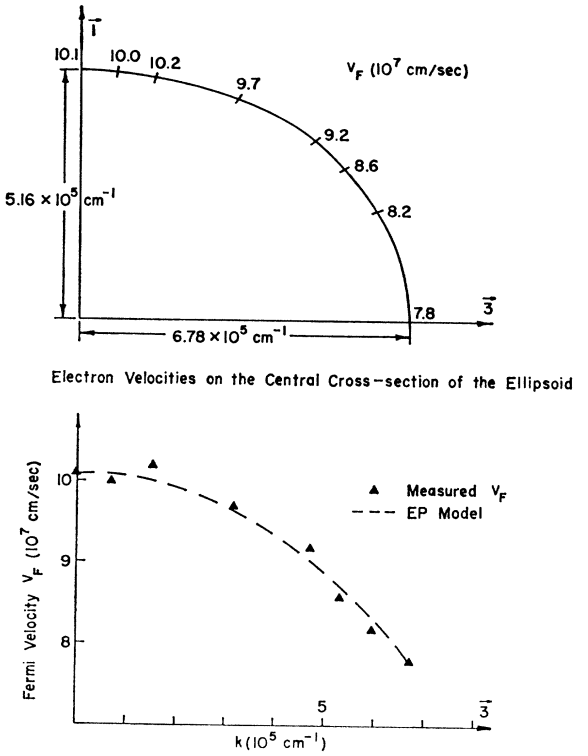

FIG. 6. Electron velocities on the (1-3) central cross section of the electron ellipsoid. The upper part of the figure shows the measured velocity values at eight different positions on a quadrant of the ellipsoid. In the lower-half is shown a plot of these velocities as a function of a the coordinate along the 3 direction of the ellipsoid, together with a calculated curve based on the EP model of the Bi band structure.

[22] J. O. Henningsen, Phys. Letters **27A**, 693 (1968).

compared. From a measurement of Doppler-shifted cyclotron resonance absorption of Alfvén waves, Edelman and Kamberski[23] derive a value of $(10.7\pm0.7)\times10^7$ cm/sec in the k_1 direction. This compares favorably with the present value of 10.1×10^7 cm/sec.

With the velocity values at hand, we are in a position to derive band mass parameters m_1 and m_3 for the EP description of the Bi energy bands. The EP model gives the velocities at points in the 1 and 3 directions as $\hbar k_1/m_1$ and $\hbar k_3/m_3$, respectively. Using the experimental values of the velocity we find

$$\begin{aligned} m_1&=\hbar k_1/v_F(0)=0.0059m_0,\\ m_3&=\hbar k_3/v_F(90)=0.010m_0, \end{aligned} \tag{21}$$

to be compared with the values of $0.0058m_0$ and $0.011m_0$ [Eq. (19)] derived from Khaikin's cyclotron mass values. The disagreement with m_3 is not unexpected. It was reflected earlier as disagreement in the calculated and experimental values of H_{12}. It is of interest to compare the present values of m_1 and m_3 with the predictions of the EP model which requires

$$k_1^2/k_3^2=m_1/m_3. \tag{22}$$

From the dimensions given by Eq. (17), we expect the ratio of masses to be $m_1/m_3=0.58$, which agrees most satisfactorily with the ratio 0.59 for the numbers that we have derived. The mass ratio using the values given in Eq. (19) is 0.53.

An alternative check on the EP model is to compare the observed variation of velocity along the elliptical section of Fig. 6 with that predicted by the model. Fitting the two endpoint velocities, we calculate the predicted variation from the EP model. The comparison (Fig. 6) of the calculated curve and the experimental values shows that the velocities follow closely the variation expected on the basis of the model.

D. Cyclotron Mass m_c

A measurement of the periodicity of the cyclotron resonance oscillations apparent in Figs. 3 and 5, determines the cyclotron mass m_c. Such measurements have been carried out in Bi by both Kao[24] and Khaikin.[21] With the magnetic field along the major axis of the ellipsoid, Kao has measured the cyclotron mass as $0.009m_0$. Khaikin's work gives $0.0081\pm0.0001m_0$, measured from the observation of as many as 20 harmonics in specimens with accurately flat surfaces. We are disturbed to find that the value of m_c from our measurements is only $0.0077\pm0.0002m_0$ and fails to agree with Khaikin's result. Our value is an average over many runs in each of the eight samples and with as many as 23 harmonics resolved. We have been careful to avoid using the high-field harmonics (for which R_c is not $\ll\delta$) in the determination of the mass. The fundamental and the next nine subharmonics have been discarded in the measurement.

There is an interesting check that we can make on the set of velocity values that we have derived. From the definition of the cyclotron mass as the line integral of the reciprocal of the velocity around the orbit, we have

$$m_c=\hbar\oint\frac{dk}{v_\perp}=\hbar\sum_i\frac{\Delta k_i}{v_{i\perp}}, \tag{23}$$

where the summation is over line segments of the elliptical section of Fig. 6. Carrying out the summation, with some interpolation between the experimental velocity values, gives $m_c=0.0077m_0$. The good agreement between the line-integral and the measured value of m_c confirms our interpretation of the surface state resonances and determination of velocity values.

E. General Aspects

The well-established Fermi-surface geometry of Bi allows us to explore and explain some of the geometrical aspects of the surface-state resonances that have been discussed by several authors.[7,10]

We begin our considerations with the case of the elongated Bi ellipsoid arranged to lie in the plane of the sample. As the magnetic field is rotated in the sample plane and away from the major axis by an angle θ, we observe a variation of the resonance fields as $1/\cos\theta$. In the case of the trigonal plane sample (which contains all three ellipsoids tilted at the small angle of 6°20′), there are found three branches of $1/\cos\theta$ curves[25] that establish clearly that the measured effect is due to the electron surfaces. We had tacitly assumed this in the previous discussions. Khaikin has shown this angular anisotropy of the data in his work on Bi,[6] and there is no need to bore the reader with a repetition of such curves. The $1/\cos\theta$ dependence is explained from a consideration of angular variation of the $(K/v^3)_\perp^{1/2}$. If we approximate the central section of the elongated ellipsoid as a cylinder with elliptical cross section, then for electrons on the zone, one finds $K=K\cos\theta$ and $v=v\cos\theta$. Combining these gives $(K/v^3)_\perp^{1/2}\propto1/\cos\theta$ and accounts for the observed angular dependence.

A second arrangement that we have examined is the case of the ellipsoid lying in the surface as previously, but with the field tilted away from the major axis and out of the sample plane. The data in a tilted field are exactly the same as data for which H is in the plane of the surface at an equal angle to the major axis. This behavior had been noted earlier in samples of Sn, In, and Al[4,5] and had been explained in terms of the cylindrical geometry of the section of the Fermi surface where the signals originate. In the case of Bi, where the central portion of the ellipsoid is an excellent approximation to the cylindrical geometry, we account for the observations in the same way. The skipping motion

[23] V. S. Edelman and V. Kamberski, in *Proceedings of the Tenth International Conference on Low-Temperature Physics, Moscow, 1966*, edited by M. P. Malkov (VINITI, Moscow, 1967), Vol. 3, p. 206.

[24] Y. H. Kao, Phys. Rev. **129**, 1122 (1963).

[25] J. D. Jensen, Ph.D. thesis, University of Maryland, 1968 (unpublished).

of the electron in real space ignores the component of field perpendicular to the cylinder axis. The electron moves in an effective field $H\cos\theta$ applied along the cylinder axis.

A more difficult case to examine is that of a cylinder (representing the central portion of the Bi ellipsoid) tilted out of the sample plane as in Fig. 7. The zone $v_z=0$ appears tilted with respect to the sample plane, and in real space the electron moves in a segment of arc that is inclined at the tilt angle θ_t relative to the surface. The cylindrical geometry, as before, implies that only the component of H in the direction of the axis determines the motion. Specular reflection of the electron in the tilted trajectory looks unusual when interpreted in terms of velocities. The tilted trajectory at incidence has a component of velocity in the y direction (parallel to the surface in our geometry) which reverses on reflection. The reflection is adequately described in terms of momentum changes $\Delta k_x=\Delta k_y=0$ and $\Delta k_z\neq 0$. With H applied along the cylinder axis, the electron moves across the zone of Fig. 7 at an angle θ_t to the surface. Upon reflection, it moves straight down by Δk_z to the lower edge of the zone. It then repeats the cycle, starting at this new point, and continues to zigzag along the zone in k space. Because of the symmetry of the cylinder, the real space motion is the same from one cycle to the next.

When a tilted ellipsoid is present, the variation of the signal, as **H** is rotated in the plane of the sample, is expected to show a minimum when the field is along the projection of the major axis. At the position of the minimum, the observed field is expected to be higher than for the case where the ellipsoid lies in the surface by the reciprocal cosine of the tilt angle. We have checked this dependence for some of the samples that had been used in the velocity studies and have found generally good agreement with the $1/\cos\theta_t$ prediction. One disconcerting exception to this rule appears to be the bisectrix (C_1) plane data. This plane has two ellipsoids, each tilted by nearly 30° out of the sample plane. The two minima in the angular variation of the data appear symmetrically on either side of the C_2 axis and are separated by 15°, as expected. We measure the minimum resonance field H_{12} as 3.58 Oe at 32.77 GHz. Scaling the in-plane value by the $1/\cos\theta_t$ factor gives 3.92 Oe. This glaring discrepancy has led us to check and recheck for possible errors in sample orientation or field readings. We are fully convinced that the missing 0.34 Oe is real, and are at a loss to explain this result. This aspect, together with all the geometrical intricacies of the three ellipsoid system, has been explored more fully in a thesis.[25]

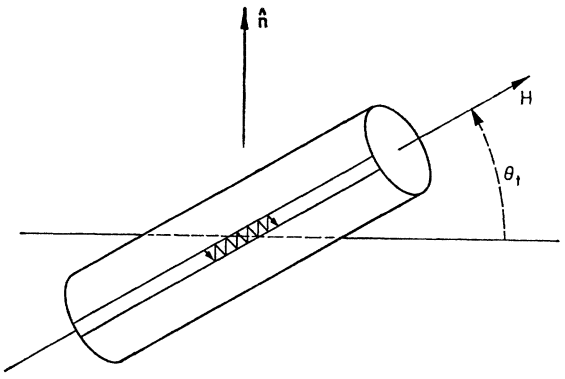

FIG. 7. Cylindrical Fermi surface tilted at angle θ_t relative to the sample surface. The skipping zone will be tilted at the same angle. With the field H along the cylinder axis electrons move along the zone in a zigzag fashion.

F. Geometry of Skipping Orbits

The derivation of the energy level scheme and our application of the formulas to evaluate the "point" velocity have assumed that the skipping electrons move only through a narrow angular range, so that $v_x\approx v_F$ and that the motion can be described by a local radius of curvature on the Fermi surface. We calculate here some of the relevant numbers to check to what extent these conditions are satisfied in Bi.

Consider for example the electron skipping about on the pointed end of the elliptical cross section shown in Fig. 6. The local radius of curvature at the midpoint of the trajectory will be $K=k_1^2/k_3=3.9\times10^5$ cm^{-1}, so that in a typical field of 3.4 Oe the corresponding cyclotron radius R is 0.76×10^{-2} cm. The maximum depth of the $n=1$ trajectory for such electrons is $z_1=0\,6\times10^{-4}$ cm, with higher state trajectories moving increasingly deeper into the metal as $(n-\frac{1}{4})^{2/3}$. It is apparent that the microwave skin depth δ in Bi is on the order of z_1; and also that both z_1 and δ are on the order of 1/100 of the cyclotron radius. This is what we had assumed in the duty-cycle argument. The length of each bounce is $2\sqrt{2}R^{1/2}z_1^{1/2}=0.96\times10^{-3}$ cm, while the half-angle of the range traversed in each cycle is nearly 7° with reference to the assumed locally circular path. Referred to the center of the elliptical section it is only 4°. At the endpoint of this particular trajectory, the curvature K will have changed by less than 1%, so that our description in terms of a locally circular path should not require serious modification. For other orbits, away from the symmetry points, the deviation in K will be larger, increasing at one end of the trajectory, decreasing on the other. Using the curvature at the midpoint of the trajectory ought to be a good approximation. Compared to a more typical metal like Cu,[12] where the electron moves only a small fraction of a degree on the Fermi surface, the case of Bi seems on the verge of breaking down the simple assumptions about the geometry of the skipping trajectories.

G. Surface Preparation

Successful observation and measurement of the surface-state resonances is crucially dependent on careful preparation of the sample surface. As we have already remarked earlier, surfaces grown on carbon-coated quartz plates barely gave observable signals. Subse-

quent electrochemical polishing made it possible to observe detailed structure and sharply resolved lines.

Polishing Bi turned out to be a haphazard adventure, and the results would vary considerably with the type of polishing procedure or such factors as polishing time, current density, age of the polishing bath, temperature and stirring rate. With a poor polish, we generally found a sharply rising baseline and only weak surface-state resonances as is evident in one of the traces of Fig. 8. Cyclotron resonance at the same time was largely unaffected. The two curves were obtained with the same crystal under identical conditions, except for the surface polish. We have also found that the samples deteriorate with time and require occasional repolishing. A systematic study of the dependence of the signals on surface preparation should reveal details of the nature of electron reflection at the surface.

VI. CONCLUDING REMARKS

The present studies of Bi represent the very first attempt to systematically use the surface-state resonance effect to explore velocities point by point over the Fermi surface of a metal. The work in Bi, because of the independently established Fermi surface parameters, also affords a critical check on the theory of surface states. In Bi, we have seen, it is possible to accurately calculate the impedance oscillation spectrum, including the k_y integration that had been ignored in previous attempts at fitting theory to experiment.[9]

While on the whole agreement of the experimental results with theoretical predictions is satisfactory, some discrepancies remain. For one, in the impedance calculations the β parameter that was necessary to fit the experimental curve, differed considerably from its calculated value based on ASE skin depth measurements. This is a serious deviation that we do not know how to resolve at present. We also admit that the signals from tilted ellipsoids are not wholly understood. We have found at least one case, where the observed peak position disagreed with the expected position outside of the possible limits of error in the experiment.

A great deal more could be done in the way of determining point velocities over other symmetry sections of the Bi ellipsoid, or for that matter at arbitrary points. The very time-consuming x-ray orientation work, and the necessity to prepare a new sample for each datum, has limited the present investigation to a single zone about the Fermi surface. It seems to us, that it would be essential to develop a more sophisticated method of making such measurements, if more detailed and complete data were desired. We would suggest using a cylindrical sample where only a small strip of the sample is exposed to the microwave radiation at one time. Rotating such a sample about its axis step by step would give the desired set of data in a single experiment.

Much of the interpretation of the resonance data in this work had to rely heavily on independently measured geometrical factors. In principle this is not really necessary. In recent studies of Cu we have been able to observe resonances in samples where the surface is cylindrically curved.[26,27] A measurement of the shift of the resonance for electrons skipping along a curved surface, determines the curvature K for that group of electrons. Combining such a measurement with a measurement of resonance fields in a flat surface sample, allows one to obtain both K and v from surface-state resonances.

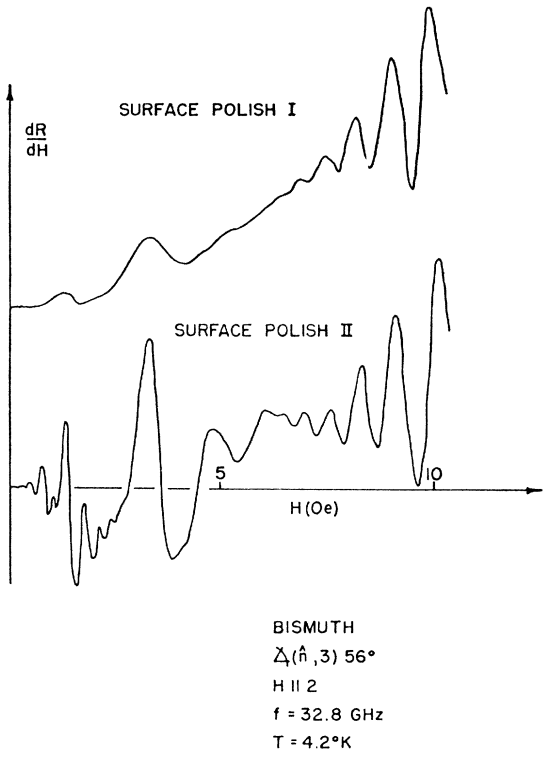

FIG. 8. Comparison of data taken on the same specimen with different surface polishes. Polish I was a poor quality electropolish, while II represents the best polish (a combination of chemical and electropolishing) ever achieved on that sample.

ACKNOWLEDGMENTS

Finally, we would like to gratefully acknowledge the collaboration with Ryan Doezema in the surface impedance calculations. Mr. Doezema has carried out the k_y integration and other computations discussed in one section of this paper. Discussions with friends and colleagues, especially R. F. Greene of the Naval Ordnance Laboratory, and R. E. Prange, T. W. Nee, and J. R. Maldonado at the University of Maryland, contributed in no small measure to the successful conclusion of this work.

[26] R. E. Prange, Phys. Rev. **171**, 737 (1968).
[27] R. E. Doezema, J. F. Koch, and U. Strom, Phys. Rev. (to be published).